JOURNAL OF MATERIALS SCIENCE 37 (2002) 3067–3074

Combined effect of fiber content and microstructure on the fracture toughness of SGF and SCF reinforced polypropylene composites

SHAO-YUN FU*, YIU-WING MAI
Centre for Advanced Materials and Technology (CAMT), Department of Mechanical and Mechatronic Engineering, J07, The University of Sydney, NSW 2006, Australia; MEEM, City University of Hong Kong, Kowloon, Hong Kong, People's Republic of China
E-mail: mesyfu@cityu.edu.hk

BERND LAUKE
Institute for Polymer Research Dresden, Hohe Str. 6, 01069 Dresden, Germany

GUANSHUI XU
Department of Mechanical Engineering, University of California, A361, Bourns Hall, Riverside, CA 92521, USA

CHEE-YOON YUE
School of Mechanical and Production Engineering, Nanyang Technological University, Nanyang Avenue, Singapore 639798

Composites of polypropylene (PP) reinforced with short glass fibers (SGF) and short carbon fibers (SCF) were prepared with extrusion compounding and injection moulding techniques. The fracture behavior of the two types of composites was studied. The fracture toughness (K_c) of the composites was measured in the T-direction [main crack transverse to mould flow direction (MFD)] and in the L-direction (main crack parallel to the MFD) using compact tension (CT) specimens made from the plaques manufactured. The study was focused on the combined effect of fiber volume fraction and microstructure (fiber length and alignment) on the fracture toughness of short fiber composites. It was observed that the addition of fibers effectively enhanced the fracture toughness for both SGF/PP and SCF/PP systems in the T-direction but only improved the composite toughness in the L-direction for the case of a low fiber volume fraction (8%). The composite fracture toughness kept almost unchanged in the T-direction and decreased in the L-direction with increasing fiber volume fraction. These were explained using the combined effect of fiber volume fraction and microstructure.

1. Introduction

Short-fiber-reinforced polymer (SFRP) composites are often made with conventional techniques, namely extrusion compounding and injection moulding, for processing polymers [1–12]. In general, a high fiber content is required to achieve a high mechanical performance SFRP composite. Thus, the effect of fiber content on the mechanical properties of SFRP composites is of particular interest. However, during processing of SFRP compounds, fiber breakage takes place. One of the major factors influencing fiber breakage is fiber-fiber interaction [13]. As fiber volume fraction increases, the interaction between fibers leads to more damage to fiber length. Thus, fiber length decreases with increasing fiber content [8]. For dumbbell shaped specimens, fibers were often aligned preferentially along the flow direction (specimen axis direction) [1, 2, 5, 6, 9]. Consequently, the tensile properties of short fiber composites will be determined both by fiber volume fraction and fiber length. Indeed, it has been shown that the tensile strength and modulus of SFRP composites are determined by the combined effect of fiber content and fiber length [9].

Studies on the effect of fiber content on the fracture toughness of SFRP composites have been carried out previously [4, 14–18]. It was observed that the composite toughness either increases or decreases as increasing fiber content [4, 14–17]. It was also noted that the fracture toughness of SFRP composites was not sensitive to fiber content [18]. The different observations are partially due to the initial different toughness values of the matrices used [4]. On the other hand, comparison of the composite fracture toughness between a shorter and a longer glass fiber reinforced composite showed that

*Author to whom all correspondence should be addressed.

the longer glass fiber reinforced composite had higher fracture toughness [17]. As pointed out above, fiber length decreases with increasing fiber content. Samples used for measurement of fracture toughness are usually made from injection moulded plaques. Fiber alignment in plaque-shaped samples varies with increasing fiber content. Thus, the effect of fiber content must be combined with the effect of microstructure, namely fiber length and fiber alignment, on the fracture toughness of SFRP composites.

In this study, polypropylene (PP) composites reinforced with short glass fibers (SGF) and short carbon fibers (SCF) were prepared with extrusion compounding and injection moulding techniques. Variation of microstructure (fiber length and alignment) in composites with increasing fiber volume fraction was discussed. The fracture toughness of SGF/PP and SCF/PP composites was studied by taking into account the combined effect of fiber volume fraction and microstructure.

2. Experimental details

The materials employed in this investigation were polypropylene (HOSTALEN PPN 1060 + 2 wt% POLYBOND 3150), E-glass fiber roving (EC 14-300-E 37 300 tex) and carbon fiber roving (TENAX HTA 5331, 800 tex). The composites were prepared by feeding glass and carbon fiber rovings into polymer melt using a twin-screw extruder. All the specimens were injection moulded into plaques under identical conditions using a twin-screw injection moulding machine with a barrel temperature of 210 to 230°C. The details about the processing have been given elsewhere [8, 9, 12]. The plaque geometry and sample orientations were shown in Fig. 1.

Compact tension (CT) testing geometry was used for the fracture tests and cracks were propagated both parallel and perpendicular to the moulding flow direction (MFD) as shown in Fig. 1. The geometry and dimensions of the CT specimens were shown in Fig. 2. The CT specimens were loaded in a static testing machine under stroke control at a constant cross-speed of 5 mm/min using 8 to 10 samples for each composition. The fracture toughness (K_c) was defined as the value of the stress intensity factor K_I at which a crack in the specimen became unstable. This occurred at a load, F_c, taken as the maximum load in the load-displacement curves. As

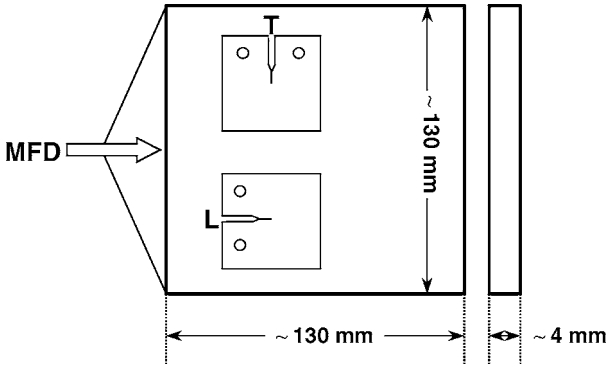

Figure 1 Macrostructure of injection-molded plaques and orientation of the compact tension test specimens.

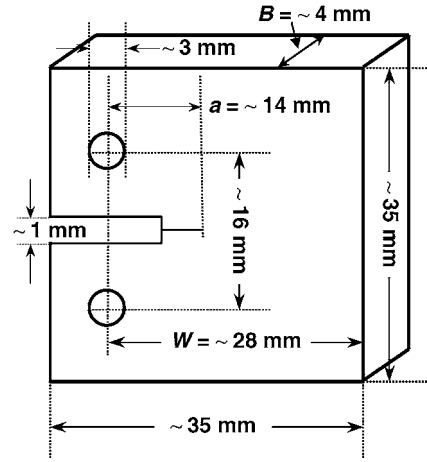

Figure 2 Geometry and dimensions of the compact tension specimens.

an approximation, the following equation was used for the calculation of K_c [4, 19]:

$$K_c = \frac{F_c}{B \cdot W} \cdot \sqrt{a} \cdot f\left(\frac{a}{W}\right) \quad (1)$$

i.e.

$$K_c = \sigma_c \cdot \sqrt{a} \cdot f\left(\frac{a}{W}\right)$$

where a is the actual crack length at the beginning of a new crack propagation test, W is the specimen width and B is the specimen thickness. $f(a/W)$ is a geometry factor for the anisotropic composite materials and is approximated by the form which is for isotropic materials

$$f\left(\frac{a}{W}\right) = 29.6 - 185.5\left(\frac{a}{W}\right) + 655.7\left(\frac{a}{W}\right)^2 - 1017\left(\frac{a}{W}\right)^3 + 639\left(\frac{a}{W}\right)^4$$

The anisotropy [considered in $f(a/W)$] may be important for certain cases which were discussed elsewhere [20]. The plaques were tested in two directions namely the T-direction and the L-direction as shown in Fig. 1 since the fiber alignment would yield highly anisotropic properties. Moreover, in order to apply Equation 1 to our case, it is necessary to justify whether the test specimens are of adequate size for generating a plane strain geometry for K_c. The specimen thickness (B) shall be larger than a minimum value, B_{min} [19]:

$$B_{min} = 2.5\left(\frac{K_c}{\sigma_y}\right)^2$$

where σ_y is a tensile yield strength. It was obtained experimentally that σ_y varies in a range of 199 MPa to 275 MPa for the composite specimens. K_c will be shown later (Fig. 3) to be lower than ~4 MPa $m^{1/2}$ for all the composite specimens. Thus, it can be easily justified that $B > B_{min}$ for all the specimens.

Fiber length measurement has been described elsewhere [8, 9, 12] and thus is briefed here. Short glass and

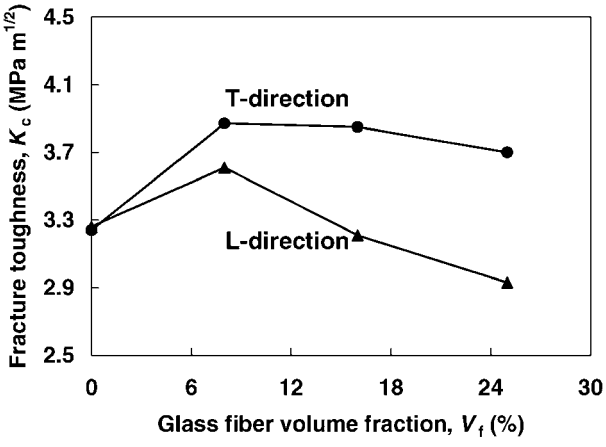

(a)

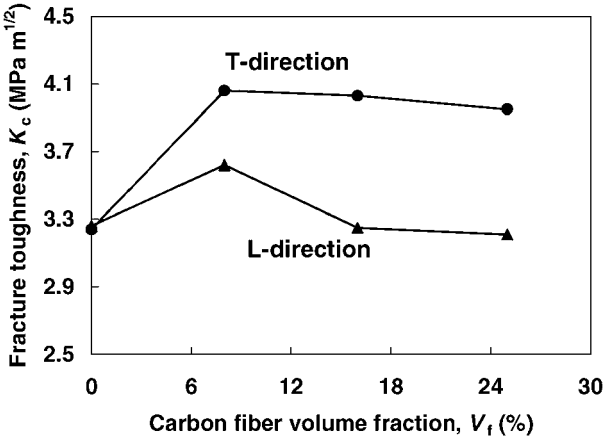

(b)

Figure 3 Fracture toughness K_c versus fiber volume fractions: (a) SGF/PP and (b) SCF/PP composites.

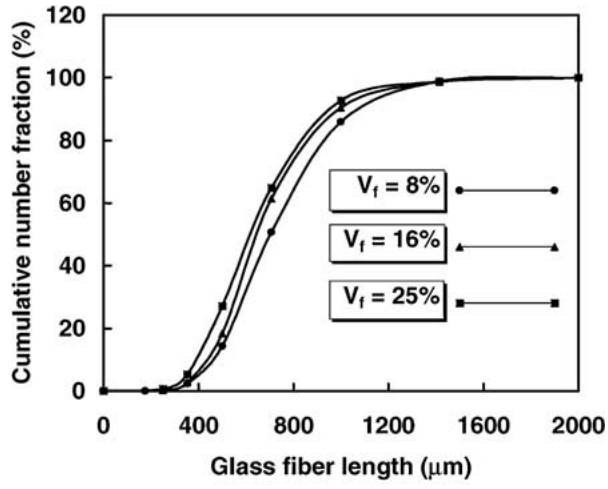

(a)

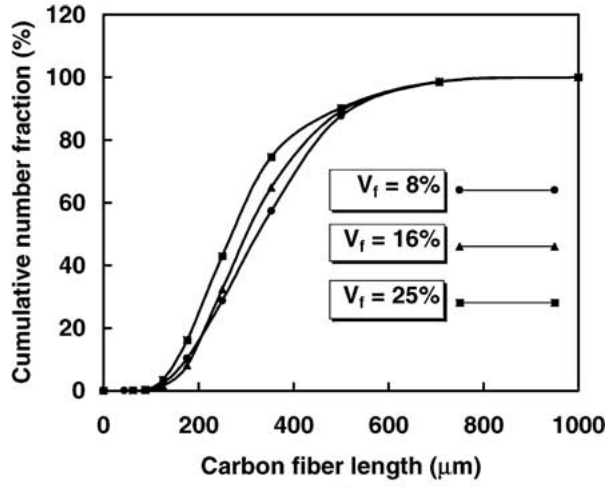

(b)

Figure 4 Cumulative glass and carbon fiber length distributions: (a) glass fiber and (b) carbon fiber.

carbon fibers were first isolated from the composite materials by pyrolysis. An ash of fibrous material was left and some fibers were extracted from the sample ash and dispersed in water in a rectangular glass dish. Magnified fiber images were transmitted to a large screen and fiber length was then determined by semi-automatically digitising with a computer.

Fractographic studies with scanning electron microscopy (SEM) were performed on the fracture surfaces of the samples. Prior to SEM observations, all fracture surfaces of the specimens were sputter-coated with gold.

Mean interfacial shear stresses for glass/polypropylene and carbon/polypropylene systems were measured using single-fiber pull-out tests and the details have been given elsewhere [8, 9]. The measured mean values of interfacial shear stresses for glass/PP and carbon/PP systems were, respectively, 15.2 MPa and 18.2 MPa. Then, the critical lengths of glass fibers and carbon fibers were obtained to be 887.92 μm and 813.87 μm, respectively [8, 9, 12].

3. Results and discussion

Glass and carbon fiber length distributions are presented in Fig. 4. It shows that fiber length distributions for both glass and carbon fibers generally shift towards the left side as fiber volume fractions increase. This is because damage to fibers increases with fiber volume fraction. Also, Fig. 4 shows that most glass fibers have a length less than their critical length ($l_c = \sim 887.92\ \mu$m) and nearly all carbon fibers are shorter than their critical length ($l_c = \sim 813.87\ \mu$m). So, most fibers would be pulled out instead of being fractured during loading of the composite when the fibers are perpendicular or moderately oblique to crack propagation directions (to be shown later in Figs 5 and 6). The effects of glass and carbon fiber volume fractions on mean glass and carbon fiber lengths are presented in Fig. 7. It can be seen that the mean glass and carbon fiber lengths decrease with increasing fiber volume fraction for both types of composites. And the mean fiber lengths are much less than the critical fiber lengths.

Plaque shaped samples of short fiber reinforced polymer (SFRP) composite usually show a three-layer structure [4, 14–18]. Schematic illustration of the 3-layer structure of the SFRP composite is shown in Fig. 8. In the skin layers, the fibers lie preferentially parallel to the MFD; in the core layer, the fibers are aligned preferentially perpendicular to the MFD. So, most fibers in the skin layers for the T-cracked samples and in the core layer for the L-cracked samples would be pulled out under loading of samples.

SEM micrographs of the fracture surfaces of the SGF/PP composites are presented in Fig. 5. For the case of the highest fiber volume fraction (25%) (see Fig. 5c), the three-layer structure can be clearly seen. And the size of the core layer is roughly 600 μm. For the cases of the lower fiber volume fraction $V_f = 8\%$ (Fig. 5a) and 16% (Fig. 5b), the three-layer structure can hardly be distinguished. That is, the core layer almost vanishes. The reduction of the core layer size (or disappearance of the core layer) can be explained as follows. The viscosity of a compounding melt affects the flow behavior and the formation of the different layers [17]. The core layer becomes thinner when the flow profile of the compounding melt is less blunted [17]. Such less blunting of the profile can be expected when the viscosity of the melt is decreased. The viscosity of a composite compounding melt increases with increasing fiber volume fraction. Hence, as fiber volume

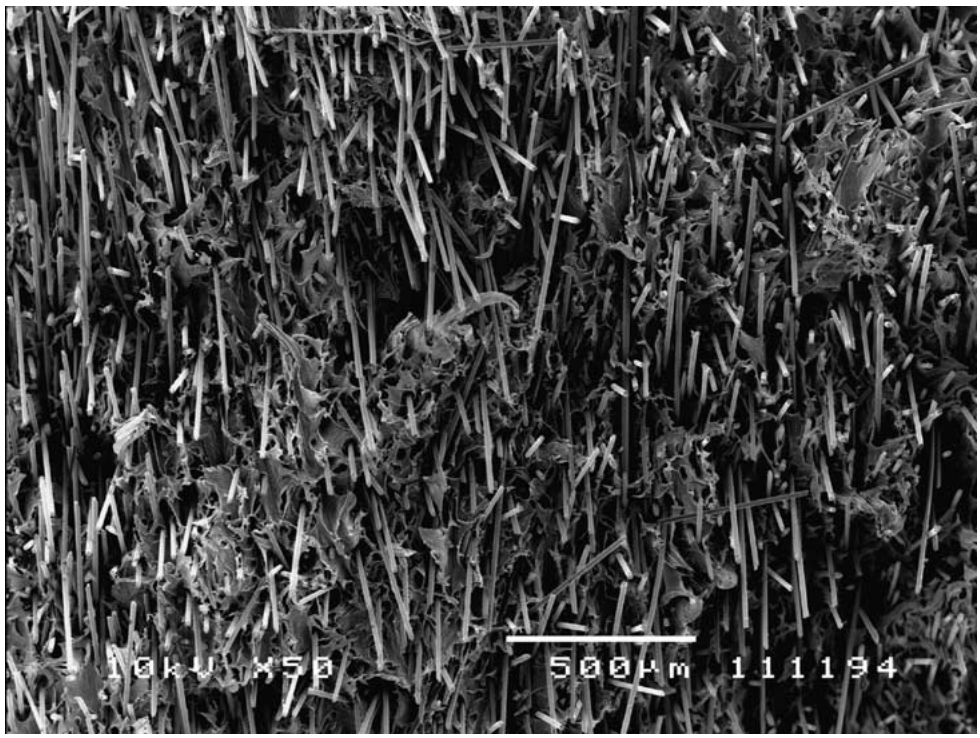

(a)

(b)

Figure 5 SEM micrographs of the fracture surfaces of the T-cracked samples for SGF/PP composites: (a) $V_f = 8\%$, (b) $V_f = 16\%$ and (c) $V_f = 25\%$. (*Continued.*)

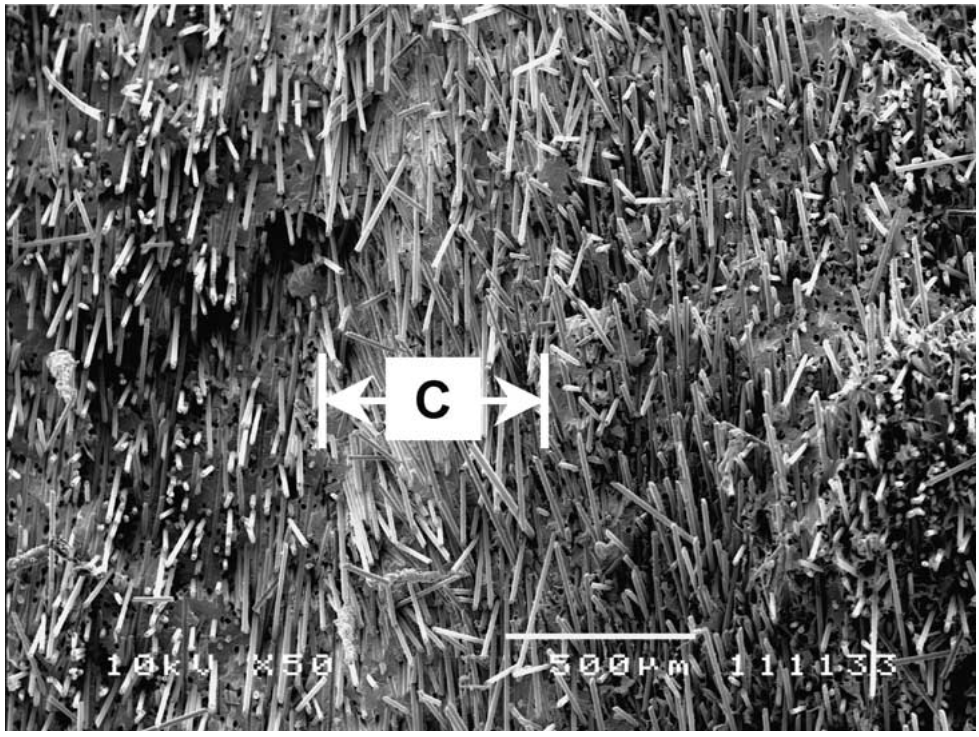

(c)

Figure 5 (*Continued.*)

fraction decreases, the viscosity of the composite compounding melt decreases. Thus, the size of the core layer decreases or even vanishes as fiber volume fraction decreases.

Comparison of fiber pull-out between the cases of 8% and 25% for SGF/PP composites is given in Fig. 6. It can be clearly seen from Fig. 6 that for the higher fiber volume fraction (25%), fiber pull-out length is much shorter than that for the lower fiber volume fraction (8%) [contrast Fig. 6a and Fig. 6b]. This is because a lower fiber volume fraction corresponds to a higher mean fiber length (see Fig. 7).

Similar SEM micrographs for SCF/PP composites were also obtained but were not presented here for simplicity. Only an exceptional case in which the matrix in the core layer fractures in a brittle manner for a carbon fiber volume fraction $V_f = 25\%$ is shown in Fig. 9.

The failure mechanisms contributing to the total composite toughness include fiber fracture, interfacial debonding, fiber pull-out and matrix fracture. The overwhelmingly dominant mechanism is fiber pull-out [4, 21]. For a short fiber composite with fiber length L shorter than critical length L_c and the fibers are transverse to crack propagation direction, fiber pull-out energy is given by [22]

$$w_{po} = \frac{V_f \tau_f L^2}{6 d_f} \tag{2}$$

where τ_f is the interfacial frictional shear stress and is assumed to be a constant. d_f is the fiber diameter. When the fibers are aligned oblique to the crack propagation direction with an angle $= 90^\circ - \theta$, the fiber pull-out energy can be derived from [22]:

$$w_{po} = \frac{V_f \tau_f L^2}{6 d_f} \exp(\mu\theta) \tag{3}$$

where μ is the snubbing frictional coefficient defined previously [23]. And μ is generally larger than zero. An assumption that the fibers are shorter than the corresponding critical length $L_{c\theta}$ of oblique fibers is made in deriving Equation 3. This is true for our cases as shown in the SEM micrographs presented since most fibers are pulled out. When $\theta = 0$, namely the fibres are perpendicular to the crack propagation direction, Equation 3 is reduced to Equation 2. Obviously the fiber pull-out energy [Equation 3] for a composite with oblique fibers is higher than that [Equation 2] for a composite with transverse fibers to the crack propagation direction. Thus, the total fracture energy of the composite with oblique fibers is higher than that of the composite with transverse fibers. From the relationship between the critical stress intensity factor (fracture toughness) K_c and the total fracture energy, it is clear that the fracture toughness of a composite with oblique fibers is higher than that for a composite with transverse fibers to the crack propagation direction. That is, the contribution of oblique fibers to the total composite toughness is larger than that of transverse fibers. In addition, it should be pointed out that the fibers parallel to the crack propagation direction do not produce any fiber pull-out energy and thus contributes much less than transverse and oblique fibers to the total composite fracture toughness.

Fracture toughness K_c versus fiber volume fractions is shown in Fig. 3. It shows that the composite toughness for the T-cracked samples is higher than that for the L-cracked samples for both types of composites. This observation is the same as reported previously

(a)

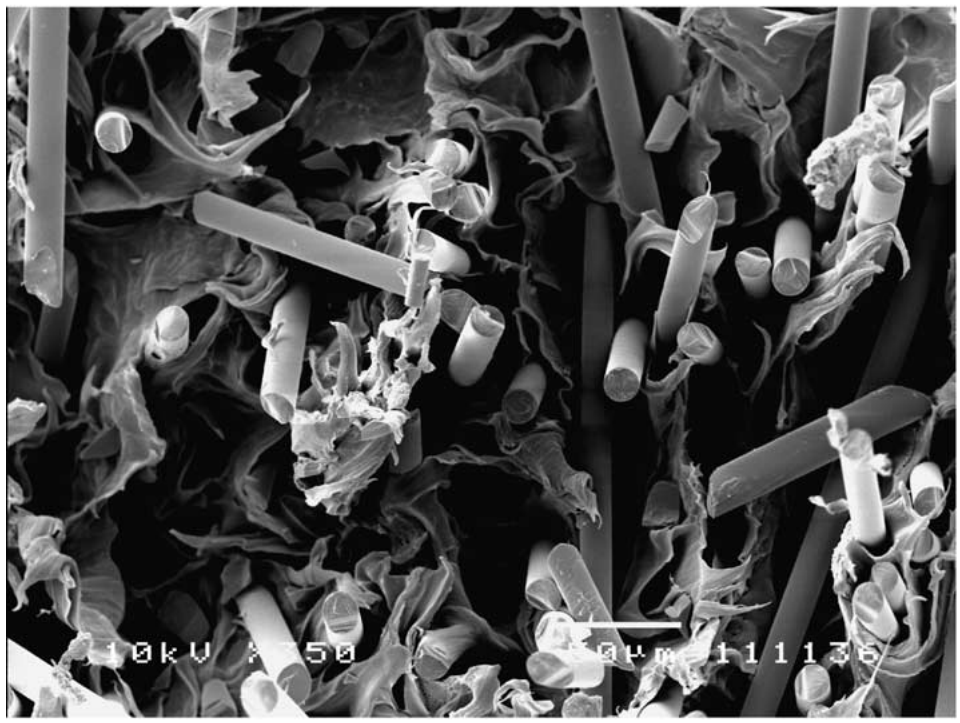

(b)

Figure 6 Comparison of the fiber pull-out at the fracture surfaces of the T-cracked samples for SGF/PP composites between (a) a lower fiber volume fraction (8%) and (b) a higher fiber volume fraction (25%).

[4, 15–17] and can be explained qualitatively as follows. The fracture toughness K_c of the composites can be evaluated by

$$K_c(V_f) = \frac{2S}{B} K_{c1}(V_f) + \frac{C}{B} K_{c2}(V_f) \qquad (4)$$

where $K_{c1}(V_f)$ is the fracture toughness of the skin layers for a given V_f; $K_{c2}(V_f)$ is the fracture toughness of the core layer. Since the size ($2S$) of the skin layers is much larger than the size (C) of the core layer, the fracture toughness of the skin layers will paly a dominant role in determining the total composite toughness. For the T-cracked samples, the fibers in the skin layers are aligned preferentially transverse (or oblique to some degree) to the crack propagation direction. For the L-cracked samples, the fibers in the skin layers are aligned preferentially parallel to the crack propagation direction. Therefore, it can be easily inferred that the fracture toughness for the T-cracked samples is higher than that for the L-cracked samples.

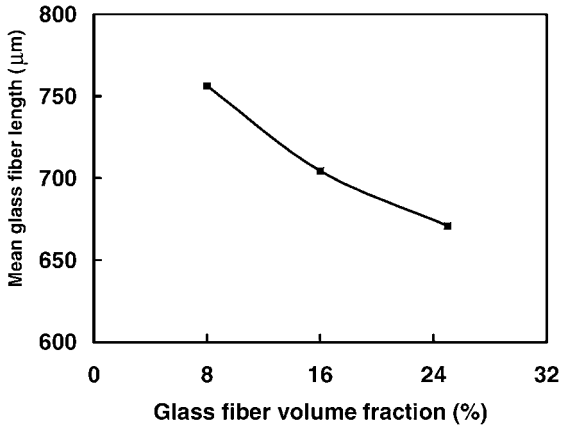

(a)

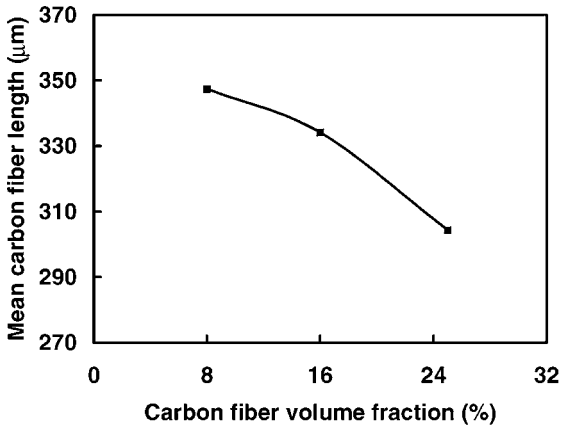

(b)

Figure 7 Mean glass and carbon fiber lengths versus fiber volume fractions: (a) glass fiber and (b) carbon fiber.

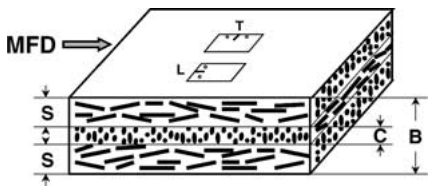

Figure 8 Schematic illustration of the three-layer structure for SFRP composite plaque samples.

Fig. 3 also shows that the addition of short fibers effectively enhances the fracture toughness for the T-cracked samples. But, the composite fracture toughness keeps almost unchanged with increasing fiber volume fraction. This can be explained by the combined effect of fiber volume fraction and microstructure. An increase in fiber content would lead to an increased fiber contribution to the total composite toughness. Conversely, as the fiber content increases, fiber length (see Figs 4 and 7) and hence fiber pull-out length (see Fig. 5) decrease. Also, the core layer, which contributes much less than the skin layers to the composite toughness, almost vanishes for the low fibre volume fractions (8% and 16%). In addition, for the case of V_f (carbon) = 25%, the matrix in the core layer does not make any contribution to the composite toughness because of the brittle fracture of the matrix (Fig. 9). Consequently, these would bring about a reduced fiber contribution to the total composite toughness as the fiber volume fraction increases. The combined effect of fiber volume fraction and microstructure would then finally lead to the almost invariant total composite toughness.

In addition, Fig. 3 shows that for the L-cracked samples, the fracture toughness is increased by the addition of SGF and SCF only for the case of the lowest fiber volume fraction (8%). For other cases, the fracture toughness is reduced by the addition of fibers. The composite toughness decreases with increasing fiber volume fraction. This can be explained as follows. It is recognized that fiber length and thus fiber pull-out length decrease with increasing fiber volume fraction. For the 8% and 16% fiber composites a certain amount of fibers are aligned oblique to the crack growth direction since the fibers are at angle to the flow direction. But, for the 25% fiber composite most fibers are aligned preferentially parallel to the crack propagation direction. These would then lead to a reduced crack resistance as fiber content increases. Thus, the composite fracture toughness decreases with the increase of fiber volume fraction for the L-cracked samples.

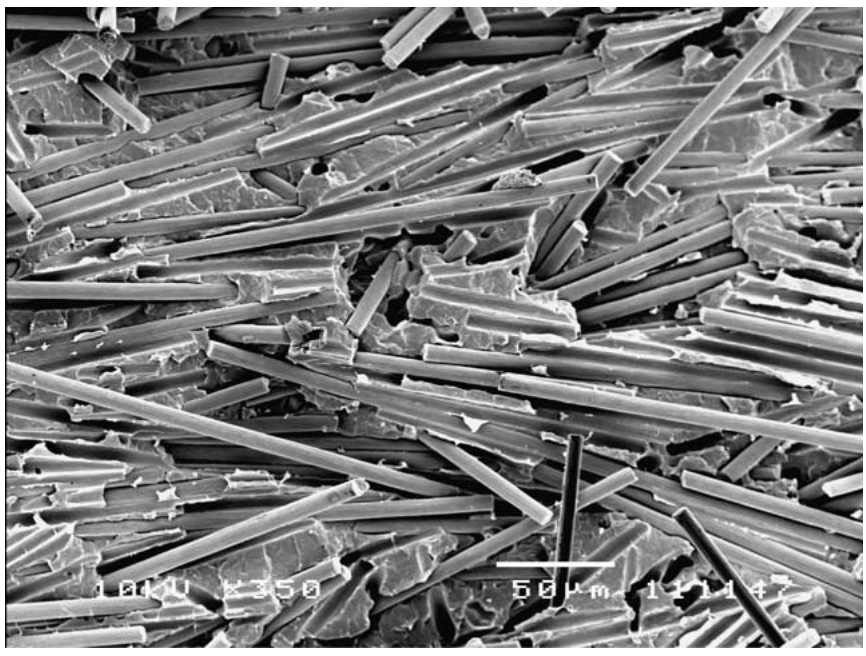

Figure 9 Brittle fracture of the matrix in the core layer for the SCF/PP composite with $V_f = 25\%$.

4. Conclusions

In this paper, the fracture behavior of injection-moulded polypropylene (PP) composites reinforced with short glass fibers (SGF) and short carbon fibers (SCF) has been studied. The microstructure (fiber length and alignment) was shown to depend on fiber volume fraction. The combined effect of fiber volume fraction and microstructure (fiber length and alignment) on the composite fracture toughness is explained. The fracture toughness of SGF/PP and SCF/PP composites was effectively enhanced for the T-cracked samples but was enhanced for the L-cracked samples only at 8 vol% by the addition of short glass and carbon fibers. Moreover, the fracture toughness of the composites was kept almost unchanged for the T-cracked samples and decreased for the L-cracked samples with the increase of fiber volume fraction. These have been explained using the combined effect of fiber content and microstructure.

References

1. M. G. BADER and J. F. COLLINS, *Fiber Sci. Technol.* **18** (1983) 217.
2. F. RAMSTEINER, *Composites* **12** (1981) 65.
3. L. BIOLZI, L. CASTELLANI and I. PITACCO, *J. Mater. Sci.* **29** (1994) 2507.
4. K. FRIEDRICH, *Compos. Sci. Technol.* **22** (1985) 43.
5. S. Y. FU and B. LAUKE, *Composites Part* A **29A** (1998) 631.
6. *Idem.*, *ibid.* **29A** (1998) 575.
7. *Idem.*, *J. Mater. Sci. Technol.* **13** (1997) 389.
8. S. Y. FU, B. LAUKE, E. MÄDER, X. HU and C. Y. YUE, *J. Mater. Process. Technol.* **89/90** (1999) 501.
9. S. Y. FU, B. LAUKE, E. MÄDER, C. Y. YUE and X. HU, *Composites Part* A **31A** (2000) 1117.
10. S. Y. FU, Y. W. MAI, B. LAUKE and C. Y. YUE, *Mater. Sci. & Engin.* A, in press.
11. P. J. HINE, R. A. DUCKETT and I. M. WARD, *Composites* **24** (1993) 643.
12. S. Y. FU, B. LAUKE, E. MADER, C. Y. YUE, X. HU and Y.-W. MAI, *J. Mater. Sci.* **36** (2000) 1243.
13. S. Y. FU, X. HU and C. Y. YUE, *Mater. Sci. Res. Intern.* **5** (1999) 74.
14. D. E. SPAHR, K. FRIEDRICH, J. M. SCHULTZ and R. S. BAILEY, *J. Mater. Sci.* **25** (1990) 4427.
15. J. KARGER-KOCSIS, *Compos. Sci. Technol.* **48** (1993) 273.
16. J. KARGER-KOCSIS and K. FRIEDRICH, *ibid.* **32** (1988) 293.
17. T. HARMIA and K. FRIEDRICH, *ibid.* **53** (1995) 423.
18. N. S. CHOI and K. TAKAHASHI, *J. Mater. Sci.* **31** (1996) 731.
19. D. BROEK, "The Practical Use of Fracture Mechanics" (Kluwer Academic Publishers, Dordrecht, The Netherlands, 1988).
20. Z. SUO, G. BAO, B. FAN and T. C. WANG, *Int. J. Solids Structures* **28** (1991) 235.
21. C. LYHMN and J. M. SCHULTZ, *J. Mater. Sci.* **18** (1983) 2029.
22. S. Y. FU and B. LAUKE, *ibid.* **32** (1997) 1985.
23. V. C. LI, Y. WANG and S. BACKER, *Composites* **21** (1990) 132.

Received 22 November 2000
and accepted 14 March 2002